AGU PUBLICATIONS

Geophysical Research Letters

RESEARCH LETTER
10.1002/2017GL073460

Key Points:
- Frictional properties of materials along the plate boundary agree with the observed slip styles
- Frictional properties of the plate boundary fault are consistent with slow slip nucleation
- The weakness of the plate boundary fault facilitates easy earthquake rupture propagation

Supporting Information:
- Supporting Information S1

Correspondence to:
M. Sawai,
msawai@chiba-u.jp

Citation:
Sawai, M., A. R. Niemeijer, T. Hirose, and C. J. Spiers (2017), Frictional properties of JFAST core samples and implications for slow earthquakes at the Tohoku subduction zone, *Geophys. Res. Lett.*, *44*, 8822–8831, doi:10.1002/2017GL073460.

Received 2 APR 2017
Accepted 22 AUG 2017
Accepted article online 29 AUG 2017
Published online 9 SEP 2017

Frictional properties of JFAST core samples and implications for slow earthquakes at the Tohoku subduction zone

Michiyo Sawai[1,2], André R. Niemeijer[3], Takehiro Hirose[1,4], and Christopher J. Spiers[3]

[1]Department of Earth and Planetary Systems Science, Graduate School of Science, Hiroshima University, Hiroshima, Japan, [2]Now at Department of Earth Sciences, Faculty of Science, Chiba University, Chiba, Japan, [3]Department of Earth Sciences, Utrecht University, Utrecht, Netherlands, [4]Kochi Institute for Core Sample Research, JAMSTEC, Nankoku, Japan

Abstract Slow earthquakes occur in the shallow (<20 km deep) part of the Tohoku subduction zone. To understand how frictional properties of the plate boundary fault affect the generation of these slow earthquakes, we conducted friction experiments using borehole samples retrieved from the plate boundary décollement and footwall during Integrated Ocean Drilling Program Expedition 343 (Japan Trench Fast Drilling Project (JFAST)). The plate boundary fault material exhibits a transition from velocity-strengthening to velocity-weakening behavior at temperatures between 50 and 150°C, which, in the framework of rate-and-state friction laws, is a necessary condition for the generation of slow earthquakes, whereas the footwall sample mainly shows velocity-strengthening behavior except at temperatures of <50°C. The downdip temperature limit of slow earthquakes in the Japan Trench also lies between 100 and 150°C. Our results suggest that the frictional properties of the plate boundary fault may play a key role in controlling the locations of observed slow earthquakes.

1. Introduction

Subduction zone earthquakes are generated by megathrust faults and may result in devastating tsunamis. On the other hand, slow earthquakes (e.g., slow slip events (SSEs), and episodic tremor and slip (ETS)) also occur throughout subduction zone regions. *Uchida et al*. [2016] reported that periodic slow slip, with repetition intervals between 1 and 6 years, is widespread in the megathrust zone of northeastern Japan. Indeed, SSEs and ETS were detected just before the 2011 Tohoku earthquake, affecting regions that seemed to include areas that slipped during the earthquake rupture [*Kato et al*., 2012; *Ito et al*., 2013] (Figure 1b). However, the cause of varying slip behavior at nearly identical pressure and temperature conditions, i.e., depth, remains unknown. To investigate this, the Integrated Ocean Drilling Program (IODP) Expeditions 343 and 343T (Japan Trench Fast Drilling Project, JFAST) successfully retrieved materials from the area of the Japan Trench plate boundary décollement that slipped during the 2011 Tohoku earthquake [e.g., *Chester et al*., 2012, 2013; *Fulton et al*., 2013] (Figure 1a). The fault zone, which was encountered at a depth of 822 m below the seafloor, is highly localized and consists of clay-rich material with a scaly fabric [*Chester et al*., 2013]. The recovered section of the scaly clay unit corresponds to about a 1 m thick fault zone. However, if we include missing intervals, the fault zone could be as thick as 4.86 m.

The frictional properties of fault gouge are one of the most important factors controlling the sliding behavior of major faults. The frictional behavior of the plate boundary material, which is derived from smectite-rich sediments of the Japan Trench, was investigated under conditions of low slip velocity by *Ikari et al*. [2015a, 2015b], and at coseismic slip velocity (~1 m/s) by *Ujiie et al*. [2013], both at room temperature. These studies revealed that the plate boundary fault zone is extremely weak and thus allows an incoming rupture to propagate easily; i.e., without much frictional dissipation of energy.

Clay minerals, and smectites in particular, are well studied, and their velocity-strengthening properties have been interpreted to be the cause of the lack of seismicity in the shallow portions (<~10 km) of subduction zones [*Logan and Rauenzahn*, 1987; *Saffer and Marone*, 2003; *Moore and Lockner*, 2004; *Ikari et al*., 2007, 2009; *Faulkner et al*., 2011; *Den Hartog et al*., 2012]. Indeed, almost all clay minerals and mixtures of clay and quartz exhibit velocity-strengthening behavior, particularly when friction is low [*Logan and Rauenzahn*, 1987; *Ikari et al*., 2009; *Tembe et al*., 2010]. However, under conditions of low normal stress and low slip velocities, the frictional properties of smectite show velocity-weakening behavior, at least at room temperature [*Saffer et al*., 2001; *Saffer and Marone*, 2003]. This all demonstrates that systematic and detailed study of

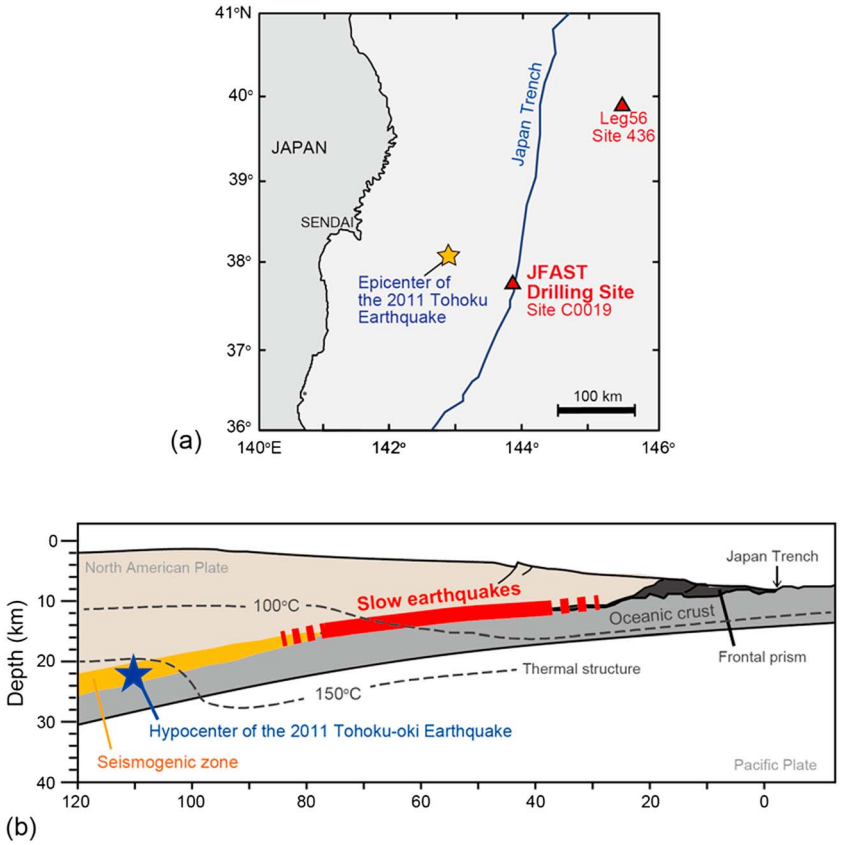

Figure 1. (a) Locations of Site C0019 (IODP Expedition 343) (JFAST) and Site 436 (DSDP Leg 56) (red triangles). Yellow star denotes the epicenter of the 2011 Tohoku earthquake, and blue line shows the Japan Trench. (b) Schematic illustration of the Tohoku subduction zone (modified from *Tsuru et al.* [2000, 2002]). The red line shows the area of slow earthquakes (*Kato et al.*, 2012; *Ito et al.*, 2013, 2015) and the yellow area indicates the seismogenic zone (*Tsuru et al.*, 2002). The hypocenter of the 2011 Tohoku earthquake is shown as a blue star, and black dashed lines indicate the isothermal lines reported by *Kimura et al.* [2012].

the frictional constitutive properties of smectite-rich gouge, under in situ conditions of effective stress and temperature, is important for understanding the stability of fault slip; i.e., whether smecite-rich fault gouge is likely to slip aseismically or has the potential to nucleate (transient) events such as slow and regular earthquakes. Since only a few studies have investigated the frictional behavior of smectite-rich gouges under various conditions of effective stress and then mostly at room temperature, we investigated the influence of temperature on frictional behavior using retrieved materials from the Japan Trench plate boundary which included an amount of clay minerals.

Since the first observations of slow slip events, more than a decade ago [e.g., *Obara*, 2002], several studies have successfully modeled their characteristics, typically within the framework of rate-and-state friction laws (RSF) [e.g., *Liu and Rice*, 2007; *Shibazaki and Shimamoto*, 2007]. Consider a simple spring-slider system in which the slider follows RSF. The instability of the system depends on the interaction between a critical stiffness K_{cr}, defined in equation (1) [*Rice and Ruina*, 1983; *Gu et al.*, 1984], and the elastic stiffness of the system K.

$$K_{cr} = \frac{-(a-b)\sigma_n^{eff}}{D_c} \tag{1}$$

where σ_n^{eff} is effective normal stress, D_c is critical slip distance and $(a-b)$ is combined parameter. Within the RSF framework, $(a-b)$ is defined as the logarithmic velocity (V) dependence of the steady state friction via the relation [*Marone*, 1998; *Scholz*, 1998]:

$$(a-b) = \frac{\partial \mu_{ss}}{\partial \ln V} \tag{2}$$

If $(a-b) \geq 0$, $K_{cr} < 0$ and the material exhibits velocity-strengthening behavior, which is intrinsically stable. On the other hand, if $(a-b) < 0$, an instability can nucleate which might lead to a dynamic event, i.e., an earthquake, depending on the departure of the critical stiffness from the stiffness of the system (equation (1)). Slip is unstable ($K < K_{cr}$) or conditionally stable ($0 < K_{cr} < K$), the latter of which represents the range of conditions thought to be most favorable for generating slow slip [*Leeman et al*., 2015, 2016]. In fact, *Leeman et al*. [2016] reported that slow slip events appeared under conditions of $K \sim K_{cr}$ in their experiments. Modeling studies showed that small but positive K_{cr} values are needed for the generation of slow slip events [e.g., *Liu and Rice*, 2007; *Shibazaki and Shimamoto*, 2007]. In the case of constant D_c, these conditions can be achieved by either small negative $(a-b)$ or negative $(a-b)$ under low effective stress. Furthermore, *Shibazaki et al*. [2010] reported that the various types of slow earthquakes (SSEs, ETS, and low-frequency earthquakes) are attained using models with varying D_c as long as the product of $(a-b)$ and σ_n^{eff} is a small negative value. Thus, it is important to investigate the variation of $(a-b)$ for the fault zone materials in the subduction zone under in situ conditions.

In this study, we investigate the frictional properties of materials cored from the plate boundary fault at the Japan Trench, under various temperature conditions. We particularly discuss how the properties change with increasing temperature; i.e., as the plate subducts into the Japan Trench, in order to understand the fault motions in the shallow part of the Tohoku subduction zone such as slow earthquakes.

2. Material and Methods

In this study, we report the results of friction experiments using smectite-rich clayey sediments and siliciclastic mud sediments derived from the Japan Trench, cored during IODP Expedition 343 of JFAST. The smectite-rich material at 822 mbsf was identified as coming from the plate boundary décollement in Core 17, collected from Site C0019 [*Chester et al*., 2012, 2013; *Kirkpatrick et al*., 2015; *Kameda et al*., 2015]. This clayey material forms a principal deformation zone, exhibiting a scaly fabric (i.e., is part of the plate boundary fault) [*Chester et al*., 2012, 2013]. The smectite-rich sediment that we used from the plate boundary décollement in Core 17 was dominated by clay minerals (approximately 91 wt %), with minor quartz and plagioclase. The undisturbed siliciclastic mud sediment we used was from Core 18, a footwall sample at 824 mbsf. Based on mineralogy and lithology, it appears to be identical to the basal sediments observed on the outer rise of the Pacific Plate, about 260 km to the northeast, at Site 436 of Leg 56 of the Deep Sea Drilling Project [*Shipboard Scientific Party*, 1980]. Our mud sample was composed mainly of clay minerals (~52 wt %) and amorphous silica (~37 wt %), with some quartz and plagioclase. The clay in cores 17 and 18 is mainly smectite, with minor illite and kaolinite, as identified by X-ray diffraction (XRD) analysis.

The samples were crushed by hand in a pestle and mortar and sieved to <125 μm to prepare simulated gouges for experiments. We prepared ring-shaped samples with inner and outer diameters of 22 and 28 mm by pressing ~0.81 g and ~0.75 g of the simulated fault gouges for Core 17 and Core 18 to obtain an initial thickness of ~1.7 mm, respectively, mixed with ~0.05 g of distilled water. This procedure allowed us to produce a relatively dense starting gouge (porosity 24%−32%), as well as to reduce loss of sample material during the experiments via extrusion. Prepressing was conducted at 50 MPa for 20 min at room temperature.

Friction experiments were performed on the simulated gouge samples using the hydrothermal ring shear apparatus at Utrecht University (described in detail by *Niemeijer et al*. [2008] and *Den Hartog et al*. [2012]) (Figure S1 in the supporting information). The ring-shaped samples were contained between two opposing, roughened Ni-superalloy pistons, with gouge layer thicknesses prior to loading of ~1.7 mm. The gouge sample was kept in place by inner and outer confining rings, which were coated with Molykote spray to reduce wall friction. After loading the vessel into the Instron frame, an effective normal stress was applied after which distilled water was added to the pore fluid system. Upon application of a small fluid pressure, rapid sample shortening was observed, which we interpret to indicate that fluid was penetrating the sample. After applying a fluid pressure, the furnace was switched on. Since the permeability of the clay-rich plate boundary fault (i.e., Core 17) was very low, below 10^{-20} m^2 [*Tanikawa et al*., 2013], the system was subsequently maintained at the desired fluid pressure and temperature and left to equilibrate for ~1 h, after which sliding was initiated by a servo-controlled motor in line with two 1:100 gearboxes. The simulated gouges were deformed at slip velocities (V) of 0.3−100 μm/s, temperatures (T) of 20–200°C, an effective normal stress (σ_n^{eff}) of 50 MPa,

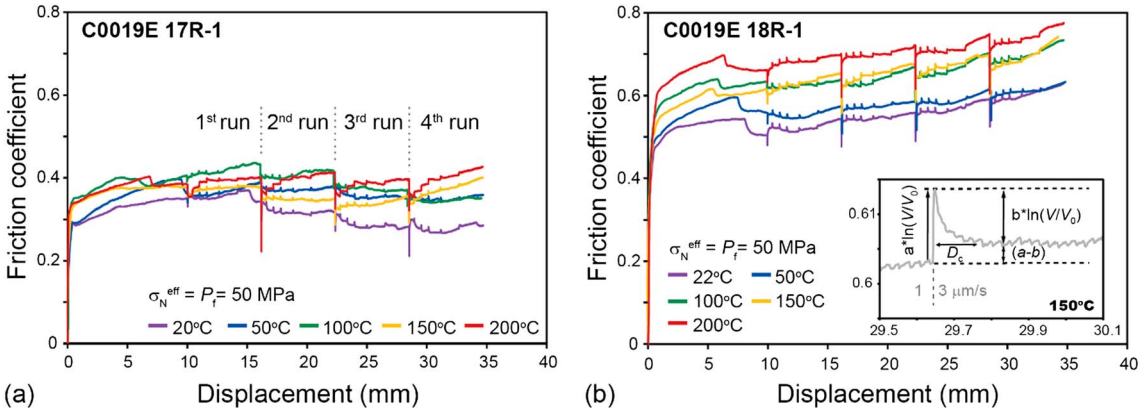

Figure 2. Friction data for borehole samples used in this study: (a and b) results for Core 17 and Core 18, respectively. Both figures show friction coefficient versus displacement in velocity-stepping tests between 0.3 and 100 μm/s under an effective normal stress and a pore fluid pressure of 50 MPa, at different temperatures. Velocity-stepping sequences were conducted four times during each experiment; these are labeled 1st run, 2nd run, 3rd run, and 4th run in Figure 2a. Inset plot in Figure 2b shows the procedure used to quantify the velocity-dependent behavior of $(a - b)$ for an experiment conducted at 150°C using the sample from Core 18.

and a fluid pressure (P_f) of 50 MPa. The temperature range includes that at the depth range in which slow slip is thought to nucleate in the Tohoku subduction zone (T = ~100°C) (Figure 1b). We set the effective normal stress equal to the pore fluid pressure so that the pore fluid factor λ was fixed ($\lambda = P_f/\sigma_n = 0.5$) in all experiments.

The samples were deformed to an initial displacement of ~10 mm at V = 10 μm/s before velocity-stepping was initiated. We repeated the same velocity-stepping sequences four times to explore the effects of shear displacement (1st−4th runs). In a single trial run, velocity-stepping tests were conducted between 0.3 and 100 μm/s to determine the rate and state parameters and to explore how they changed with temperature and slip velocity. The velocity dependence of the friction was assumed to be described by the RSF laws [*Dieterich*, 1978, 1979; *Ruina*, 1983]:

$$\mu = \mu_0 + a \ln\left(\frac{V}{V_0}\right) + b \ln\left(\frac{V_0\theta}{D_c}\right), \qquad \text{with} \quad \frac{d\theta}{dt} = 1 - \frac{V\theta}{D_c} \tag{3}$$

where μ is the instantaneous coefficient of friction, μ_0 is a reference coefficient of friction at a reference velocity V_0, θ is a state variable, and D_c is a characteristic slip distance. To determine the parameters a, b, and D_c, we used the inversion technique described by *Saffer and Marone* [2003]. Data analysis was performed using the XLook program developed at Pennsylvania State University.

3. Results

Table S1 lists the key data pertaining to each experiment. The experimental conditions and the apparent friction coefficient μ (i.e., shear stress divided by effective normal stress, ignoring cohesion) versus displacement data obtained in each experiment are shown in Figure 2. The apparent friction coefficient ranges from 0.31 to 0.38 for Core 17 (67% smectite) and from 0.55 to 0.70 for Core 18 (38% smectite), thus increasing with decreasing smectite content. In both samples, especially in Core 18, the values of μ tend to increase with increasing temperature.

The parameter $(a - b)$ varies with increasing temperature. In Core 17, $(a - b)$ increases from negative values at ≤100°C to positive values at 200°C (Figures 3a−3c and S2a−S2e), except at postslip velocities (i.e., velocities after each velocity stepping) of 30 μm/s and 100 μm/s. At the highest postslip velocities, the $(a - b)$ versus temperature curve exhibits U-shaped behavior: it decreases from positive at 20°C to negative values at 100°C and then returns to positive values at 200°C. In contrast, $(a - b)$ for Core 18 tends to increase with increasing temperature, from negative or neutral to positive values, at all slip velocities (Figures 3g−3i and S2f−S2j).

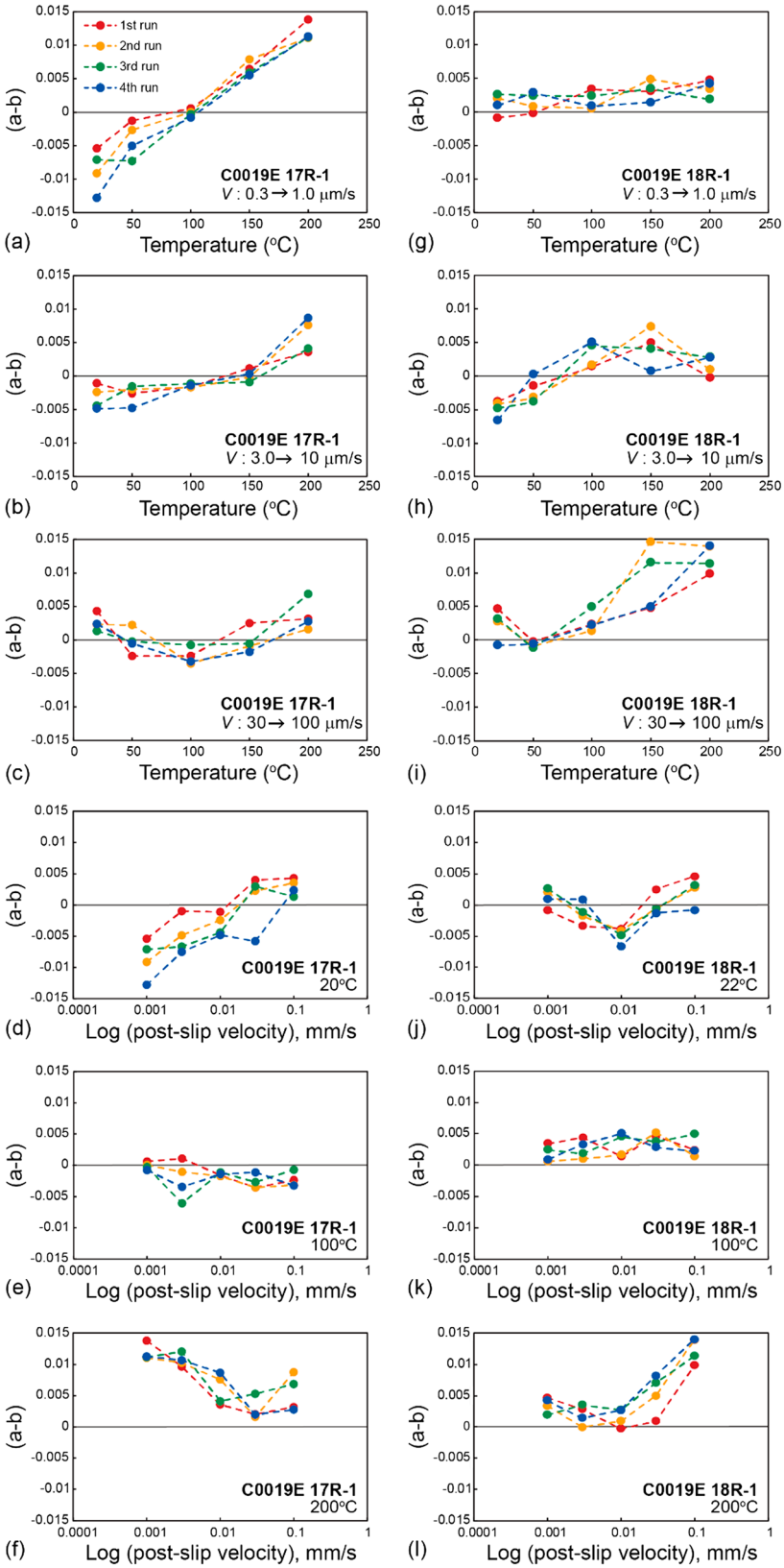

Figure 3. Frictional velocity dependence ($a - b$) as a function of temperature and slip velocity under an effective normal stress and a pore fluid pressure of 50 MPa. (a–f) Representative values of parameter ($a - b$) for the sample from Core 17 at postslip velocities of 1.0, 10, and 100 μm/s (Figures 3a–3c) and at temperatures of 20, 100, 200°C (Figures 3d–3f). (g–l) Corresponding representative values for the sample from Core 18.

In Core 17, at a temperature of 20°C, ($a - b$) clearly increases with increasing slip velocity to 100 μm/s. However, it remains roughly constant at temperatures of 50−100°C and decreases with increasing slip velocity at temperatures >150°C (Figures 3d−3f and S3a−S3e), eventually returning to negative values. In Core 18, variations of ($a - b$) with slip velocity are more complex. At 22°C, ($a - b$) decreases from positive (or near zero) at a postslip velocity of 1 μm/s to negative values at 10 μm/s, but it returns to near zero or positive values at a postslip velocity of 100 μm/s (Figures 3j and S3f). The parameter ($a - b$) exhibits the same trend at 50°C, although the minimum value of ($a - b$) shifts to a higher postslip velocity of 30 μm/s. At temperatures higher than 100°C, most ($a - b$) values are positive and increase with increasing slip velocity.

The constitutive parameters a, b, and D_c of cores 17 and 18 are plotted as functions of temperature in Figures S4 and S5, respectively. In both samples, as temperature increases, a increases and b decreases. Like ($a - b$), the dependence of the individual parameters on slip velocity is complex (Figures S6 and S7). Parameter a appears to increase with increasing ($a - b$) and decrease with decreasing ($a - b$); values of b increase with decreasing ($a - b$) and decrease with increasing ($a - b$). In contrast, D_c does not vary systematically with temperature or slip velocity in the investigated experimental range.

4. Discussion and Conclusions

Ikari et al. [2015a] conducted friction experiments on JFAST borehole samples under effective normal stresses of 5−7 MPa at room temperature. The plate boundary fault material and wall rock samples they used were composed of ~70% and ~15–20% smectite (in the bulk sediment), respectively. They reported that plate boundary fault material was weak (μ = 0.20−0.26) in contrast to the wall rocks ($\mu > 0.5$). Our results of plate boundary material (i.e., Core 17) and footwall material (i.e., Core 18) at temperatures of 20°C and 22°C, respectively, are consistent with their observations (Figure 2). The difference in observed frictional strength is most likely the result of differences in smectite content. The smectite-rich fault zone retrieved from the plate boundary thrust during JFAST (i.e., Core 17) was highly localized [*Chester et al*., 2012, 2013; *Kirkpatrick et al*., 2015]. Weak plate boundary fault rock, with relatively strong footwall material, likely make it energetically favorable for earthquake ruptures to propagate along the plate boundary, thus producing the observed 1 m thick (maximum thickness 4.86 m), highly localized region of deformation within the fault zone.

It is widely accepted that clay minerals, including smectites, mainly exhibit velocity-strengthening behavior, although some previous studies have reported that smectite at room temperature exhibits velocity-weakening behavior at low slip velocities (<20 μm/s) under conditions of low normal stress (<40 MPa) [*Saffer et al*., 2001; *Saffer and Marone*, 2003]. Smectite retains variable amounts of water within the interlayer space (one- to three-layer hydrates) [*Sposito and Prost*, 1982]. Hydrated smectites can show either velocity-weakening or velocity-strengthening behavior; negative and positive ($a - b$) values are associated with low (1−3 μm/s) and high (100−300 μm/s) slip velocities, respectively [*Saffer and Marone*, 2003; *Ikari et al*., 2007], whereas water-saturated samples generally exhibit velocity strengthening [e.g., *Tembe et al*., 2010]. Although we did not explore the role of fluid saturation state within gouge layers, our results revealed that the clay-rich plate boundary fault shows velocity-weakening behavior under a range of combinations of temperature and slip velocity. Indeed, velocity-weakening occurs not only at low (room) temperature and low slip velocity, in agreement with previous studies, but also at elevated temperatures (100−150°C) with a high slip velocity (100 μm/s; Figures 3, S2, and S3). Although the values of ($a - b$) change from negative to positive as slip velocity increases at room temperature, this trend gradually disappears as the temperature increases (Figures 3d−3f and S3a−S3e). Furthermore, the opposite trend appears at temperatures >150°C, and ($a - b$) values become positive at all velocities explored at 200°C (Figures 3d−3f and S3a−S3e). Thus, the frictional behavior of the fault is complex, and it changes as a function of both temperature and slip velocity, at a fixed effective stress of 50 MPa.

Gouge layer thickness data sometimes provide clues about the possible mechanisms affecting the velocity dependence of friction [e.g., *Samuelson et al*., 2009]. For example, dilatancy of fault gouge may cause velocity-strengthening behavior by depressurizing of the internal pore fluid (dilatancy hardening) [*Segall and Rice*, 1995]. In the present study, however, no clear trend is observed in dilatation with increasing slip velocity or temperature. The physical processes underlying such complex frictional behavior, including that seen in our results, are still unknown and further experiments, including detailed microstructural observations, are clearly needed.

Variations in (a–b) inevitably reflect variations in the friction parameters a and/or b. In Cores 17 and 18, a increases and b decreases, while the value of ($a - b$) increases. Negative ($a - b$), i.e., velocity-weakening behavior, is thus caused by a decrease in a and an increase in b (Figures S2–S7), which shows a similar dependence to the parametric changes reported by *Ikari et al*. [2009] for clay-rich fault gouge. *Scholz* [2002] suggested that changes in b reflect the evolution of the contact area over time, while *Saffer and Marone* [2003] suggested that near-zero values of b resulted from a complete contact of clay gouge surfaces implying a zero change in the true contact area upon velocity steps (contact saturation). The contact area of smectite may become saturated as temperature increases. The direct effect a is believed to be due to the rate dependence of the shear strength of contact points [*Dieterich and Kilgore*, 1994] and has been inferred to increase with increasing temperature [*Sleep*, 1997]. *Blanpied et al*. [1998] reported values of a obtained from frictional experiments on granite gouge and showed that they tend to increase with temperature. In the present study, a also tends to increase with increasing temperature. This may indicate a change in the rate dependence of direct contact strength or perhaps an increase in a cohesive strength component of contacts.

In the framework of RSF, fault instability depends on stiffness K and critical stiffness K_{cr}, as defined in (1). As mentioned in section 1, *Shibazaki et al*. [2010] reported that the slow earthquakes can be reproduced using models with varying D_c as long as the product of ($a - b$) and σ_n^{eff} is a small negative value. In the case of this study, the effective normal stress is constant, and the experimental D_c values that we obtained were almost constant (<0.6 mm). This means that the conditions of a small, negative ($a - b$) values, believed to favor the initiation of slow earthquakes, are most likely to be met, in our data, at temperatures where ($a - b$) is negative or zero at a transition from velocity-weakening to strengthening. Most of episodic tremor and slow slip events have been recorded in the shallow portion of the Japan Trench (<20 km), where temperatures lie between about 50°C and 150°C, based on the thermal structure. Our results from Core 17 show a transition between velocity-weakening and strengthening behavior with increasing temperature, which leads to the parameter ($a - b$) taking the small negative values believed to promote slow slip in the temperature range 50–150°C, at all slip velocities investigated (Figures 3a−3c and S2a−S2e). This transition in ($a - b$) is key for generating slow earthquakes, and the corresponding temperature range identified in our experiments shows good agreement with the depth range in which slow earthquakes are observed in the Japan Trench regions (Figure 1b).

Our experiments have focused on the effect of temperature and accordingly suggest that it may indeed be the temperature-dependent frictional properties of the plate boundary fault that facilitate the nucleation of slow earthquakes. However, the effective normal stress might be another key parameter. *Saffer and Marone* [2003] have reported that the values of ($a - b$) for smectite change from negative to positive with increasing normal stress at room temperature, and *Scuderi and Collettini* [2016] have shown that the parameter ($a - b$) for carbonate gouges changes with increasing pore fluid pressure at room temperature. Some studies have investigated the effective normal stress dependence at temperatures in the range 22–400°C. Phyllosilicate-rich samples, taken from the Alhamade Murcia Fault in Spain, showed a large change in ($a - b$) over in situ ranges of effective stress and temperature [*Niemeijer and Vissers*, 2014]. Similarly, *Den Hartog and Spiers* [2013] and *Sawai et al*. [2016] showed that the sensitivity of ($a - b$) to effective normal stress in experiments on illite-quartz and blueschist gouges varied clearly with temperature. Thus, the sensitivity of ($a - b$) to effective normal stress probably does display a temperature dependence in phyllosilicates, and more experiments on smectite-rich samples are needed to address this.

The inference on the frictional properties of materials along the plate boundary, based on experimental data, has important implications for the nucleation of megathrust earthquakes and slow earthquakes in the Tohoku subduction zone (Figure 4). *Sawai et al*. [2016] reported that blueschist fault rocks, which are likely to be present at seismogenic depths in the Tohoku subduction zone, showed velocity-weakening behavior at temperatures characterizing the seismogenic zone. By comparing their results, and combining with the results of the present work, we can extrapolate their insights to the frictional properties of the entire plate boundary fault. The resulting evolution of the rate and state parameter ($a - b$) under a given effective normal stress (σ_n^{eff} = 50 MPa), for both the plate boundary fault and blueschist, is shown in Figure 4a. Since smectite, which is the main mineral in Core 17, should dehydrate as it is subducted, frictional data from the clay-rich plate boundary fault (i.e., Core 17) are adopted up to 100°C. Experimental results for blueschist are used for the deeper part.

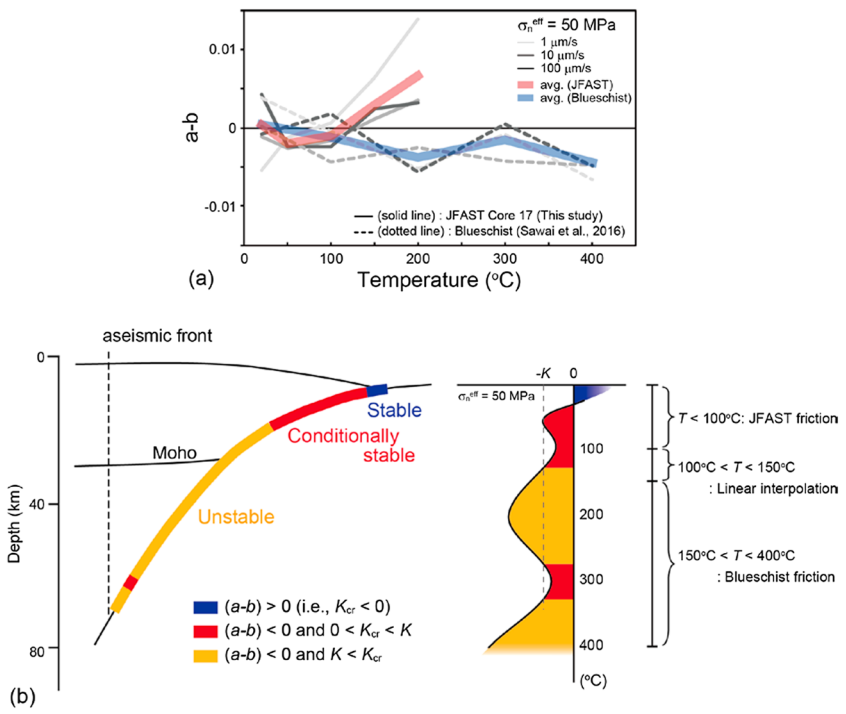

Figure 4. Frictional properties of plate boundary materials based on experiments on plate boundary fault samples taken from the Tohoku subduction zone (this study) and blueschist (*Sawai et al.*, 2016). (a) Values of ($a - b$) versus temperature for JFAST Core 17 (solid lines) and blueschist (dotted lines). All data plotted correspond to results obtained at an effective normal stress of 50 MPa, a pore fluid pressure of 50 MPa, and postslip velocities of 1.0, 10, and 100 μm/s, in order to compare the results and combine the data from both blueschist and Core 17. Red and blue lines are average values at $\sigma_n^{eff} = P_f = 50$ MPa for Core 17 and blueschist, respectively. The results shown for Core 17 are from the first run only because blueschist samples were not repeated the velocity-stepping sequences (i.e., velocity-stepping tests were conducted only once at each pressure-temperature condition). (b) Schematic illustration of the evolution of the frictional properties, based on experimental results shown in Figure 4a. Left figure in Figure 4b shows a cross section of the subduction zone based on the geothermal gradient reported by *Peacock and Wang* [1999]. Right figure in Figure 4b shows a possible $-K_{cr}$ versus temperature curve based on the experiments. Note that the friction of JFAST Core 17 in Figure 4b is applied at $T < 100$°C, blueschist friction is applied at $T > 150$°C, and friction in the temperature range 100°C $< T <$ 150°C is considered as an interpolation zone.

Based on these results, a conceptual model for the Tohoku subduction zone is proposed in Figure 4b. This model agrees with the generation of the various observed slip styles shown in Figure 1b, although this model should depend on the fault zone stiffness, K, in the Tohoku subduction zone. Stable slip occurs without an earthquake just under the seafloor, while the potentially unstable area, the model shows, agrees with the seismogenic zone observed in the Tohoku subduction zone (Figure 1b) [*Tsuru et al.*, 2002]. In the shallow portion at less than ~20 km, our model indicates conditionally stable behavior, which includes the potential for slow earthquakes, and slow earthquakes are indeed detected at this area (Figure 1b) [*Kato et al.*, 2012; *Ito et al.*, 2013, 2015]. The model also shows conditionally stable behavior in the deep portions of Tohoku subduction zone although it should depend on the fault zone stiffness, K. The possible K_{cr} for around 300°C is negative so would be capable of generating regular earthquakes but also predicts a tendency for slow earthquakes in some cases; to date, there have been no observations of them. In the present approach based on experimental data, friction in the temperature range 100°C–150°C is considered to be an interpolation zone. *Den Hartog and Spiers* [2014] reported that a microphysical model that predicts the onset of velocity-weakening behavior at around 140°C, at a slip velocity of 10^{-9} m/s, i.e., below lab velocities toward plate velocities, using otherwise equivalent conditions to the experiments on illite-quartz gouge. Their result agrees well with the updip seismogenic limit on subduction megathrusts and shows the transition back to velocity-strengthening occurring at 193°C. Thus, there is also the possibility that transitions from smectite to illite and from illite to blueschist occur at 100–150°C and at 150–200°C, respectively. The model we suggest does not change much even if illite-quartz data are used at around 150°C. Thus, our results suggest that the frictional properties of materials at the plate boundary do seem to be one of the important factors in controlling slip instability and earthquake generation.

Acknowledgments
We would like to express our sincere thanks to Marco M. Scuderi, an anonymous reviewer, and the Associate Editor Ake Fagereng for careful and constructive review which improved our paper. This study used samples and data provided by the Integrated Ocean Drilling Program (IODP). We appreciate the advice of Colin Peach when using the Utrecht ring shear instrument. Technical support in maintaining the ring shear machine was provided by T. van der Gon Netscher, G. Kastelein, and E. de Graaff. We also thank Osamu Tadai (Kochi Institute for Core Sample Research, JAMSTEC) for help with conducting XRD analyses. This study was/is supported by a Grant-in-Aid for JSPS Fellows (to M.S.), and by JSPS KAKENHI grant 16H04064 (to T.H.). A.R.N. is supported by European Research Council starting grant SEISMIC (335915) and the Netherlands Organization for Scientific Research (NWO) VIDI grant 854.12.011.

References

Blanpied, M. L., C. J. Marone, D. A. Lockner, J. D. Byerlee, and D. P. King (1998), Quantitative measure of the variation in fault rheology due to fluid-rock interactions, *J. Geophys. Res.*, *103*, 9691–9712, doi:10.1029/98JB00162.

Chester, F. M., J. J. Mori, S. Toczko, N. Eguchi, and the Expedition 343/343T Scientists (2012), Japan trench Fast drilling project (JFAST), IODP Prel. Rept., 343/343T, doi:10.2204/iodp.pr.343343T.2012.

Chester, F. M., et al. (2013), Structure and composition of the plate-boundary slip zone for the 2011 Tohoku-Oki earthquake, *Science*, *342*(6163), 1208–1211, doi:10.1126/science.1243719.

Den Hartog, S. A. M., and C. J. Spiers (2013), Influence of subduction zone conditions and gouge composition on frictional slip stability of megathrust faults, *Tectonophysics*, *600*, 75–90, doi:10.1016/j.tecto.2012.11.006.

Den Hartog, S. A. M., and C. J. Spiers (2014), A microphysical model for fault gouge friction applied to subduction megathrusts, *J. Geophys. Res. Solid Earth*, *119*, 1510–1529, doi:10.1002/2013JB010580.

Den Hartog, S. A. M., A. R. Niemeijer, and C. J. Spiers (2012), New constraints on megathrust slip stability under subduction zone P-T conditions, *Earth Planet. Sci. Lett.*, *353–354*, 240–252, doi:10.1016/j.epsl.2012.08.022.

Dieterich, J. H. (1978), Time-dependent friction and the mechanics of stick-slip, *Pure Appl. Geophys.*, *116*, 790–806.

Dieterich, J. H. (1979), Modeling of rock friction: 1. Experimental results and constitutive equations, *J. Geophys. Res.*, *84*, 2161–2168, doi:10.1029/JB084iB05p02161.

Dieterich, J. H., and B. D. Kilgore (1994), Direct observation of frictional contacts: New insights for state-dependent properties, *Pure Appl. Geophys.*, *143*, 283–302.

Faulkner, D. R., T. M. Mitchell, J. Behnsen, T. Hirose, and T. Shimamoto (2011), Stuck in the mud? Earthquake nucleation and propagation through accretionary forearcs, *Geophys. Res. Lett.*, *38*, L18303, doi:10.1029/2011GL048552.

Fulton, P. M., et al. (2013), Low coseismic friction on the Tohoku-Oki fault determined from temperature measurements, *Science*, *342*(6163), 1214–1217, doi:10.1126/Science.1243641.

Gu, J. C., J. R. Rice, A. L. Ruina, and T. T. Simon (1984), Slip motion and stability of a single degree of freedom elastic system with rate and state dependent friction, *J. Mech. Phys. Solids*, *32*(3), 167–196.

Ikari, M. J., D. M. Saffer, and C. Marone (2007), Effect of hydration state on the frictional properties of montmorillonite-based fault gouge, *J. Geophys. Res.*, *112*, B06423, doi:10.1029/2006JB004748.

Ikari, M. J., D. M. Saffer, and C. Marone (2009), Frictional and hydrologic properties of clay-rich fault gouge, *J. Geophys. Res.*, *114*, B05409, doi:10.1029/2008JB006089.

Ikari, M. J., Y. Ito, K. Ujiie, and A. J. Kopf (2015a), Spectrum of slip behaviour in Tohoku fault zone samples at plate tectonic slip rates, *Nat. Geosci.*, *8*, 870–874, doi:10.1038/ngeo2547.

Ikari, M. J., J. Kameda, D. M. Saffer, and A. J. Kopf (2015b), Strength characteristics of Japan trench borehole samples in the high-slip region of the 2011 Tohoku-Oki earthquake, *Earth Planet. Sci. Lett.*, *412*, 35–41, doi:10.1016/j.epsl.2014.12.014.

Ito, Y., et al. (2013), Episodic slow slip events in the Japan subduction zone before the 2011 Tohoku-Oki earthquake, *Tectonophysics*, *600*, 14–26, doi:10.1016/j.tecto.2012.08.022.

Ito, Y., R. Hino, S. Suzuki, and Y. Kaneda (2015), Episodic tremor and slip near the Japan Trench prior to the 2011 Tohoku-Oki earthquake, *Geophys. Res. Lett.*, *42*, 1725–1731, doi:10.1002/2014GL062986.

Kameda, J., M. Shimizu, K. Ujiie, T. Hirose, M. Ikari, J. Mori, K. Oohashi, and G. Kimura (2015), Pelagic smectite as an important factor in tsunamigenic slip along the Japan Trench, *Geology*, *43*, 155–158, doi:10.1130/G35948.1.

Kato, A., K. Obara, T. Igarashi, H. Tsuruoka, S. Nakagawa, and N. Hirata (2012), Propagation of slow slip leading up to the 2011 M_W 9.0 Tohoku-Oki earthquake, *Science*, *335*, 705–708, doi:10.1126/science.1215141.

Kimura, G., S. Hina, Y. Hamada, J. Kameda, T. Tsuji, M. Kinoshita, and A. Yamaguchi (2012), Runaway slip to the trench due to rupture of highly pressurized megathrust beneath the middle trench slope: The tsunamigenesis of the 2011 Tohoku earthquake off the east coast of northern Japan, *Earth Planet. Sci. Lett.*, *339–340*, 32–45, doi:10.1016/j.epsl.2012.04.002.

Kirkpatrick, J. D., et al. (2015), Structure and lithology of the Japan Trench subduction plate boundary fault, *Tectonics*, *34*, 53–69, doi:10.1002/2014TC003695.

Leeman, J., M. M. Scuderi, C. Marone, and D. Saffer (2015), Stiffness evolution of granular layers and the origin of repetitive, slow, stick-slip frictional sliding, *Granular Matter*, *17*(4), 1–11, doi:10.1007/s10035-015-0565-1.

Leeman, J. R., D. M. Saffer, M. M. Scuderi, and C. Marone (2016), Laboratory observations of slow earthquakes and the spectrum of tectonic fault slip modes, *Nature*, *7*, 11104, doi:10.1038/ncomms11104.

Liu, Y., and J. R. Rice (2007), Spontaneous and triggered aseismic deformation transients in a subduction fault model, *J. Geophys. Res.*, *112*, B09404, doi:10.1029/2007JB004930.

Logan, J. M., and K. A. Rauenzahn (1987), Frictional dependence of gouge mixtures of quartz and montmorillonite on velocity, composition, and fabric, *Tectonophysics*, *144*, 87–108.

Marone, C. (1998), Laboratory-derived friction laws and their application to seismic faulting, *Annu. Rev. Earth Planet. Sci.*, *26*, 643–696, doi:10.1146/annurev.earth.26.1.643.

Moore, D. E., and D. A. Lockner (2004), Crystallographic controls on the frictional behavior of dry and water-saturated sheet structure minerals, *J. Geophys. Res.*, *109*, B03401, doi:10.1029/2003JB002582.

Niemeijer, A. R., and R. L. Vissers (2014), Earthquake rupture propagation inferred from the spatial distribution of fault rock frictional properties, *Earth Planet. Sci. Lett.*, *396*, 154–164.

Niemeijer, A. R., C. J. Spiers, and C. J. Peach (2008), Frictional behaviour of simulated quartz fault gouges under hydrothermal conditions: Results from ultra-high strain rotary shear experiments, *Tectonophysics*, *460*, 288–303, doi:10.1016/j.tecto.2008.09.003.

Obara, K. (2002), Non-volcanic deep tremor associated with subduction in southwest Japan, *Science*, *296*, 1679–1681, doi:10.1126/science.1070378.

Peacock, S. M., and K. Wang (1999), Seismic consequences of warm versus cool subduction metamorphism: Examples from southwest and northeast Japan, *Science*, *286*, 937–939, doi:10.1126/science.286.5441.937.

Rice, J. R., and A. L. Ruina (1983), Stability of steady frictional slipping, *J. Appl. Mech.*, *50*(2), 343–349.

Ruina, A. (1983), Slip instability and state variable friction laws, *J. Geophys. Res.*, *88*, 10,359–10,370, doi:10.1029/JB088iB12p10359.

Saffer, D. M., and C. Marone (2003), Comparison of smectite- and illite-rich gouge frictional properties: Application to the updip limit of the seismogenic zone along subduction megathrusts, *Earth Planet. Sci. Lett.*, *215*, 219–235, doi:10.1016/S0012-821X(03)00424-2.

Saffer, D. M., K. M. Frye, C. Marone, and K. Mair (2001), Laboratory results indicating complex and potentially unstable frictional behavior of smectite clay, *Geophys. Res. Lett.*, *28*, 2297–2300, doi:10.1029/2001GL012869.

Samuelson, J., D. Elsworth, and C. Marone (2009), Shear-induced dilatancy of fluid-saturated faults: Experiment and theory, *J. Geophys. Res.*, *114*, B12404, doi:10.1029/2008JB006273.
Sawai, M., A. R. Niemeijer, O. Plümper, T. Hirose, and C. J. Spiers (2016), Nucleation of frictional instability caused by fluid pressurization in subducted blueschist, *Geophys. Res. Lett.*, *43*, 2543–2551, doi:10.1002/2015GL067569.
Scholz, C. H. (1998), Earthquakes and friction laws, *Nature*, *391*, 37–42, doi:10.1038/34097.
Scholz, C. H. (2002), *The Mechanics of Earthquakes and Faulting*, 2nd ed., Cambridge Univ. Press, New York.
Scuderi, M. M., and C. Collettini (2016), The role of fluid pressure in induced vs. triggered seismicity: Insights from rock deformation experiments on carbonates, *Sci. Rep.*, *6*, 24852, doi:10.1038/srep24852.
Segall, P., and J. R. Rice (1995), Dilatancy, compaction, and slip instability of a fluid-infiltrated fault, *J. Geophys. Res.*, *100*, 22,155–22,171, doi:10.1029/95JB02403.
Shibazaki, B., and T. Shimamoto (2007), Modelling of short-interval silent slip events in deeper subduction interfaces considering the frictional properties at the unstable-stable transition regime, *Geophys. J. Int.*, *171*, 191–205, doi:10.1111/j.1365-246X.2007.03434.x.
Shibazaki, B., S. Bu, T. Matsuzawa, and H. Hirose (2010), Modeling the activity of short-term slow slip events along deep subduction interfaces beneath Shikoku, southwest Japan, *J. Geophys. Res.*, *115*, B00A19, doi:10.1029/2008JB006057.
Shipboard Scientific Party (1980), Site 436, Japan Trench Outer Rise, Leg 56, in *Scientific Party*, *Initial Reports of the Deep Sea Drilling Project*, *56*, *57*, Pt. 1, Washington, D. C., U.S. Govt. Printing Office, pp. 399–446, doi:10.2973/dsdp.proc.5657.107.1980.
Sleep, N. H. (1997), Application of a unified rate and state friction theory to the mechanics of fault zones with strain localization, *J. Geophys. Res.*, *102*, 2875–2895, doi:10.1029/96JB03410.
Sposito, G., and R. Prost (1982), Structure of water adsorbed on smectites, *Chem. Rev.*, *82*(6), 553–573.
Tanikawa, W., T. Hirose, H. Mukoyoshi, O. Tadai, and W. Lin (2013), Fluid transport properties in sediments and their role in large slip near the surface of the plate boundary fault in the Japan Trench, *Earth Planet. Sci. Lett.*, *382*, 150–160, doi:10.1016/j.epsl.2013.08.052.
Tembe, S., D. A. Lockner, and T.-F. Wong (2010), Effect of clay content and mineralogy on frictional sliding behavior of simulated gouges: Binary and ternary mixtures of quartz, illite, and montmorillonite, *J. Geophys. Res.*, *115*, B03416, doi:10.1029/2009JB006383.
Tsuru, T., J. Park, N. Takahashi, S. Kodaira, Y. Kido, Y. Kaneda, and Y. Kono (2000), Tectonic features of the Japan trench convergent margin off Sanriku, northeastern Japan, revealed by multichannel seismic reflection data, *J. Geophys. Res.*, *105*, 16,403–16,413, doi:10.1029/2000JB900132.
Tsuru, T., J. Park, S. Miura, S. Kodaira, Y. Kido, and T. Hayashi (2002), Along-arc structural variation of the plate boundary at the Japan Trench margin: Implication of interplate coupling, *J. Geophys. Res.*, *107*(B12), 2357, doi:10.1029/2001JB001664.
Uchida, N., T. Iinuma, R. M. Nadeau, R. Bürgmann, and R. Hino (2016), Periodic slow slip triggers megathrust zone earthquakes in northeastern Japan, *Science*, *351*(6272), 488–492.
Ujiie, K., et al. (2013), Low coseismic shear stress on the Tohoku-Oki megathrust determined from laboratory experiments, *Science*, *342*(6163), 1211–1214, doi:10.1126/science.1243485.